Volume 147
Number 6
21 March 2022
Pages 977-1246

Analyst

rsc.li/analyst

ISSN 0003-2654

ROYAL SOCIETY OF CHEMISTRY

COMMUNICATION
Tsuyoshi Minami *et al.*
Oxytocin detection at ppt level in human saliva by an extended-gate-type organic field-effect transistor

Analyst

ROYAL SOCIETY OF CHEMISTRY

COMMUNICATION

View Article Online
View Journal | View Issue

Cite this: *Analyst*, 2022, **147**, 1055

Received 3rd December 2021,
Accepted 15th February 2022

DOI: 10.1039/d1an02188e

rsc.li/analyst

Oxytocin detection at ppt level in human saliva by an extended-gate-type organic field-effect transistor†

Kohei Ohshiro, [a] Yui Sasaki, [a] Qi Zhou, [a] Xiaojun Lyu, [a] Yusuke Yamanashi,[b] Katsumasa Nakahara,[b] Hirokazu Nagaoka[b] and Tsuyoshi Minami *[a]

Herein, we report an extended-gate-type organic field-effect transistor (OFET) sensor for oxytocin. The fabricated OFET-based immunosensor has successfully detected oxytocin at a ppt level in human saliva with high recovery rates (96–102%). We believe our sensor would pave the way for the realization of portable sensors for healthcare monitoring.

Oxytocin yielded in neurosecretory neurons is a representative peptide hormone consisting of nine types of amino acid residues, which plays a crucial role in biological systems as a neurotransmitter.[1] To date, versatile roles of oxytocin as an anabolic bone hormone,[2,3] an age-specific circulating hormone,[4] medicine for chronic abdominal pain,[5] *etc.* in peripheral tissue have been reported. In addition, the psychological association with peripheral effects of oxytocin has also been vigorously investigated, whereas the mechanisms in biological systems are still unclear.[6,7] Therefore, easy-to-detection of oxytocin can facilitate fundamental research in the fields of diagnosis, maternity nursing, pharmacology, and molecular biology. In particular, quantitative detection of oxytocin levels in human saliva would be an indicator to monitor the relationship between psychological changes and peripheral effects.[8] Oxytocin has been conventionally analyzed utilizing large analytical apparatuses (*e.g.*, liquid chromatography-mass spectrometry (LC-MS)[9–11] and capillary electrophoresis,[12,13] while such methods have considerable issues such as the requirement of expensive large instruments and trained personnel, and time-consuming. In the context of the above, the development of a rapid and facile sensing system is desirable.

As a sensing platform for oxytocin detection, we have focused on an organic field-effect transistor (OFET).[14] By employing appropriate organic semiconductors, the OFET devices can be easily fabricated utilizing high-throughput printable methods (*e.g.*, robotic dispensers and inkjet printers[15–17]). Furthermore, the OFETs enable molecular recognition combined with detection portions (*e.g.*, enzymes,[18–21] antibodies,[18,22] molecularly imprinted polymers,[23–25] and artificial receptors[26,27]), allowing electrical detection in aqueous media. Among them, the potential changes at an interface of a separated-gate electrode (connected to the OFET) and an analyte solution, which are induced by the capturing of charged chemical species, vary the conductance of the OFET. Thus, modifying the detection portion on the gate electrode can endow the OFET devices with molecular detectability.[28–30] Indeed, we firstly detected various chemical species including anions,[21,31] amino acids,[23] and proteins[15,32] in aqueous media using the extended-gate-type OFETs. However, the realization of OFET-based hormone sensors is still in its infancy. To this end, we designed the printable extended-gate-type OFET for oxytocin detection and applied it for real sample analysis in human saliva (Fig. 1).

Toward ultra-sensitive and selective oxytocin detection, an immunosensing method has been employed.[9] Notably, we have succeeded in the functionalization of the antibody-

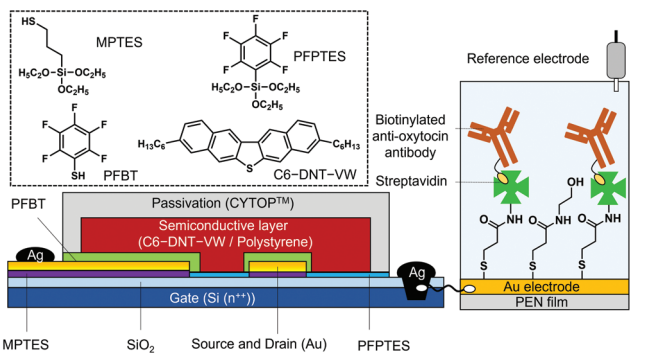

Fig. 1 Schematic illustration of the extended-gate-type OFET sensor for oxytocin detection.

[a]*Institute of Industrial Science, The University of Tokyo, 4-6-1 Komaba, Meguro-ku, Tokyo, 153-8505, Japan. E-mail: tminami@iis.u-tokyo.ac.jp*
[b]*JNC Petrochemical Corp., 5-1, Goikaigan, Ichihara, Chiba, 290-8551, Japan*

† Electronic supplementary information (ESI) available: The details of materials, measurements, fabrication process and characterization results (CV, PYS, wettability test, and basic characteristics) of the oxytocin sensor, OFET measurements, and real sample analysis by SVM. See DOI: 10.1039/d1an02188e

attached self-assembled monolayer (SAM) on the extended-gate electrodes for chemical sensing.[15,32] A short alkyl chain-based SAM could contribute to the highly sensitive detection based on chemical sensing within Debye length.[33] In this regard, amide bonds of the SAM could form intermolecular hydrogen bonds, which allow uniform membrane even with short alkyl chains. Moreover, a modified streptavidin on the SAM has been utilized to immobilize a biotinylated anti-oxytocin antibody through biotin–avidin interaction.[34,35] The changes in transistor characteristics by chemical sensing significantly depend on the alignment status of charge distribution on the extended-gate electrode.[15] In other words, the well-ordered immobilization of the antibody by the biotin–streptavidin could allow the accurate and reproducible detection of oxytocin. Based on the above strategic design, we successfully quantified oxytocin at ppt levels (equivalent to pg mL^{-1}) in human saliva with the extended-gate-type OFET functionalized with the biotinylated-oxytocin antibody.

The extended-gate-type OFET possessing an operation part (*i.e.*, OFET) and a sensing portion (*i.e.*, extended gate) was designed for chemical sensing in aqueous media.[32] As shown in Fig. 1, the newly designed OFET on a silicon substrate (*i.e.*, Si (n^{++})) consists of SiO_2 as a gate dielectric, gold (Au) as source and drain, and 3,9-dihexyldinaphtho[2,3-*b*:2,3-*d*]thiophene (C6-DNT-VW)[36] as a semiconductor. The p-type semiconductive material, C6-DNT-VW was employed because of high solubility in various types of organic solvents, resulting in the high-throughput printing process by the robotic dispenser system. In this study, a mixture of C6-DNT-VW and polystyrene was applied to obtain reproducible uniform semiconductive layer.[37] For an interfacial chemical treatment between the silicon substrate and the Au electrode, (3-mercaptpropyl) triethoxysilane (MPTES) was utilized to facilitate the ability of adhesion at the interface of different materials.[38] Moreover, the channel region was fully coated with triethoxy(pentafluorophenyl)silane (PFPTES) to increase hydrophobicity for printing the organic semiconductive layer. Furthermore, the Au electrode was treated using pentafluorobenzenethiol (PFBT) for alleviation of carrier injection barriers between the Au electrode and the organic semiconductive layer.[39] Finally, a fluorinated polymer (*i.e.*, CYTOP™) was spin-coated onto the OFET to passivate the organic semiconductive layer. The gate electrode of the OFET and the extended gate functionalized with the oxytocin detection scaffold were connected by a copper cable, and gate voltage (V_{GS}) was applied from an Ag/AgCl reference electrode.

The transistor characteristics upon the addition of chemical species were evaluated under ambient conditions using a semiconductor parameter analyzer. A constant drain voltage (V_{DS} = −1 V) was applied to the drain electrode, and the sweep voltage (V_{GS}) was applied to the gate electrode from 0.5 V to −3 V for transfer characteristics. The V_{DS} was swept from 0 V to −3 V, while V_{GS} was set from 0 V to −3 V at |1| V steps for output characteristics. The OFET was stably operated under the low-voltage conditions even in several repetitive measurements, indicating that the fabricated OFET can be used as a chemical sensor for molecular detection in aqueous solutions (Fig. S7, ESI†). Further details of the fabrication process and electrical measurements were described in the ESI.†

As the sensing part, we fabricated an oxytocin detection portion on a flexible plastic film (*i.e.*, polyethylene naphtalate (PEN)) toward ultra-sensitive and selective detection of oxytocin. The Au electrode was firstly treated with 3-mercaptopropionic acid. Subsequently, the coupling reaction using *N*-hydroxysulfosuccinimide and *N*,*N*′-diisopropylcarbodiimide was carried out to form the amide bond on the extended-gate electrode. Next, streptavidin was modified on the obtained monolayer, followed by immobilization of the biotinylated anti-oxytocin antibody through the biotin–streptavidin interaction.[40] The step-by-step functionalized electrodes were evaluated by linear sweep voltammetry (LSV),[41] photoelectron yield spectroscopy (PYS) measurements in air[42] and wettability measurements.

The Au electrode modified by 3-mercaptopropionic acid was characterized to estimate the density of the monolayer using LSV, which resulted in (3.1 ± 0.1) × 10^{-9} mol cm^{-2} (Fig. S3, ESI†). The reproducible uniform monolayer was successfully obtained on the extended-gate electrode even though the short-alkyl chain for the linker unit. Next, PYS measurements showed a deeper work function of the treated Au electrode by 3-mercaptopropionic acid (5.10 ± 0.02 eV) than that of the untreated Au electrode (4.69 ± 0.04 eV), which was probably due to an electronegative functional group originating from 3-mercaptopropionic acid-based monolayer on the Au electrode. In this regard, results of the wettability investigation exhibited a drastic change in contact angels on the Au electrodes from 51 ± 2.0° to 6.4 ± 0.5° based on the modification of 3-mercaptopropionic acid. In contrast, no photoelectric effect in the PYS measurement was observed by the streptavidin-immobilized electrode because the surface of the electrode was presumably fully covered by the protein (Fig. S4 and S5, ESI†). As shown, step-by-step modification of SAM on the extended-gate electrode was successfully evaluated, the electrode combined with the OFET was thus applied to electrical detection.

With the characterized electrode, the modification of anti-oxytocin antibody was subsequently performed in Dulbecco's phosphate-buffered saline (D-PBS) solution containing Tween 20 (0.05 wt%) and human serum albumin (HSA) (0.1 wt%) at 37 °C. As shown in Fig. S8(A),† transfer characteristics of the OFET displayed a gradual negative shift with increasing the antibody concentration up to 50 μg mL^{-1}, indicating that the biotinylated antibody was immobilized on the streptavidin-modified electrode. Next, the OFET-based chemical sensor was applied to oxytocin detection, the response time of which was saturated at most within 10 min. The OFET functionalized with the anti-oxytocin antibody negatively shifted upon the addition of oxytocin (Fig. 2(A)), and the corresponding titration isotherm exhibited a non-linear curve that implied successful quantitative detection (Fig. 2(B)). Indeed, a negligible change in a subthreshold swing with (0.24 ± 0.01 mV dec^{-1}) was observed even in nine times repetitive measurements, while

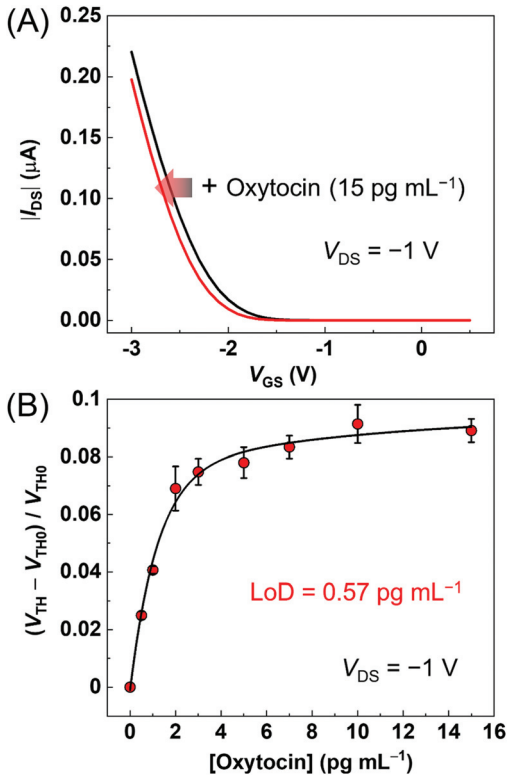

Fig. 2 (A) Transfer characteristics of the biotinylated anti-oxytocin antibody modified OFET upon the addition of oxytocin in D-PBS buffer solution containing Tween 20 (0.05 wt%) and human serum albumin (0.1 wt%). (B) Titration isotherm of the oxytocin detection. [Oxytocin] = 0–15 pg mL^{-1}. The errors at 0–15 pg mL^{-1} were 3–12%.

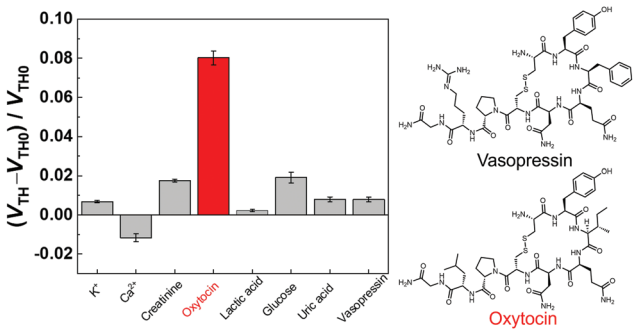

Fig. 3 Result of the selectivity test against eight types of chemical species (*i.e.*, D-glucose (10 μg mL^{-1}), creatinine (0.3 μg mL^{-1}), L-lactic acid (18 μg mL^{-1}), uric acid (8 μg mL^{-1}), potassium ion (K^+) (547 μg mL^{-1}), calcium ion (Ca^{2+}) (48 μg mL^{-1}), vasopressin (10 pg mL^{-1}), and oxytocin (10 pg mL^{-1})).

the transfer curves negatively shifted upon the addition of charged species. Thus, the observed negative shift attributed to the changes in carrier concentration in the OFET channel affected by the charged species (*i.e.*, oxytocin) on the extended-gate electrode.[43] Very importantly, the limit of detection (LoD) was estimated to be 0.57 pg mL^{-1} according to the 3σ method,[44] which suggested that the OFET successfully detected oxytocin with high sensitivity even in the presence of the excess amount of interferents (Fig. 2(B)). Certainly, the estimated LoD was overwhelmingly lower than other detection methods such as enzyme immunoassay or optical sensor devices (Table S1, ESI†), which implied the capability of the OFET-based sensor for practical detection in human saliva at a physiologically normal range (0–10 pg mL^{-1}).[45,46] Furthermore, the selectivity test was performed using eight types of chemical species containing in saliva (*i.e.*, D-glucose (10 μg mL^{-1}), creatinine (0.3 μg mL^{-1}), L-lactic acid (18 μg mL^{-1}), uric acid (8 μg mL^{-1}), potassium ion (K^+) (547 μg mL^{-1}), calcium ion (Ca^{2+}) (48 μg mL^{-1}), vasopressin (10 pg mL^{-1}), and oxytocin (10 pg mL^{-1})). Among them, vasopressin showing a chemical structural similarity with oxytocin[1] was employed to evaluate the discriminability of the OFET-based sensor. Fig. 3 obviously displayed the highest response of the OFET to oxytocin (10 pg mL^{-1}), which suggested that the OFET-based sensor succeeded in selective detection of oxytocin.

As the next trial, we performed oxytocin detection in artificial saliva. To prepare the artificial saliva, D-glucose (10 μg mL^{-1}), creatinine (0.3 μg mL^{-1}), L-lactic acid (18 μg mL^{-1}), uric acid (8 μg mL^{-1}), and albumin (1.78 mg mL^{-1}) were additionally added into artificial medical saliva (Saliveht Aerosol) to mimic human saliva. Even in such a complicated environment, the transfer characteristics of the OFET shifted toward a negative direction with increasing oxytocin concentration as shown in Fig. S16.† Thus, we decided to apply the oxytocin sensing system for real sample analysis to examine the detectability of the OFET-based sensor in real-world scenarios.

The real sample analysis was carried out using human saliva sample taken from a healthy volunteer that was authorized by the Ethics Committee of the University of Tokyo (ethics authorization code: 20-108). Informed consent was obtained for any experimentation with human subjects. The step-wise shift of transistor characteristics was observed upon the addition of oxytocin at the range of 0–50 pg mL^{-1} in human saliva, and the non-linear titration curve corresponding to V_{TH} changes was thus obtained (Fig. 4(A)). The LoD in human saliva was determined to be 3.9 pg mL^{-1}. For a spike recovery test, a calibration line was established by a linear least-squares method using a dataset of transistor characteristics collected in artificial saliva. The values of the root-mean-square errors of calibration (RMSEC) and prediction (RMSEP) represent the accuracy of the built calibration model and its predictive capacity. The estimated recovery values using human saliva at 20 and 25 pg mL^{-1} showed 96% and 102% (n = 3) (Table S2, ESI†), which implied the highly accurate analytical results by the OFET-based sensor (Fig. 4(B)). In this regard, a regression analysis provided a low value of RMSEP in Fig. S17,† indicating that the OFET-based sensor enabled the prediction of unknown concentrations of oxytocin with high accuracy. Given the fact that the oxytocin levels of pregnant and lactating women's saliva (10–40 pg mL^{-1}),[47] the OFET would be applied to practical diagnostics.

In summary, we designed the facile chemical sensor using OFET for oxytocin toward highly sensitive and selective detec-

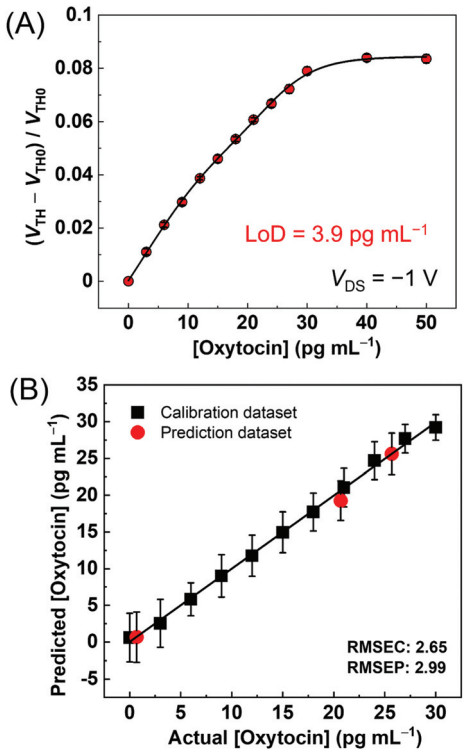

Fig. 4 (A) Titration isotherm of the oxytocin detection in human saliva at pH = 7.5. [Oxytocin] = 0–50 pg mL^{-1}. The errors at 0–50 pg mL^{-1} were 2–12%. (B) Spike recovery test for oxytocin using human saliva.

tion. The uniform anti-oxytocin antibody-attached SAM on the extended-gate electrode allowed reproducible detection. With the functionalized extended-gate electrode, the OFET quantitatively responded to oxytocin even in the presence of the excess amount of interferents. Moreover, the anti-oxytocin-antibody modified OFET showed the discriminatory power of slightly different chemical structures of hormones. Furthermore, the OFET-based sensor achieved accurate oxytocin detection with a low LoD value (0.57 pg mL^{-1}). Furthermore, the spike recovery test in human saliva achieved 96% and 102% of recovery rates, revealing that the high detectability of the OFET-based oxytocin sensor in real-world scenarios. Importantly, many layers of the OFET were fabricated by wet processes, meaning that the OFET would be fabricated by using printing methods such as inkjet printers.[15] We believe that our proposed sensor based on organic electronics would pave the way for the realization of portable hormone sensors.

Author contributions

KO fabricated the OFET device, investigated the OFET performance. YS wrote the manuscript. QZ carried out the electrochemical experiments. XL carried out the data analysis for the spiked recovery test. YY, KN and HN contributed to the device fabrication. TM conceived the entire project.

Conflicts of interest

The authors declare no competing financial interest.

Acknowledgements

TM thanks JSPS KAKENHI (Grant No. JP21H01780, JP20K21204, and JP20H05207) and JST CREST (Grant No. JPMJCR2011), and New Energy and Industrial Technology Development Organization (NEDO) (Grant No. JPNP14012).

References

1 R. M. Buijs, *Pharmacol. Ther.*, 1983, **22**, 127–141.
2 R. Tamma, G. Colaianni, L.-l. Zhu, A. DiBenedetto, G. Greco, G. Montemurro, N. Patano, M. Strippoli, R. Vergari, L. Mancini, S. Colucci, M. Grano, R. Faccio, X. Liu, J. Li, S. Usmani, M. Bachar, I. Bab, K. Nishimori, L. J. Young, C. Buettner, J. Iqbal, L. Sun, M. Zaidi and A. Zallone, *Proc. Natl. Acad. Sci. U. S. A.*, 2009, **106**, 7149–7154.
3 C. S. Carter, W. M. Kenkel, E. L. MacLean, S. R. Wilson, A. M. Perkeybile, J. R. Yee, C. F. Ferris, H. P. Nazarloo, S. W. Porges, J. M. Davis, J. J. Connelly and M. A. Kingsbury, *Pharmacol. Rev.*, 2020, **72**, 829–861.
4 C. Elabd, W. Cousin, P. Upadhyayula, R. Y. Chen, M. S. Chooljian, J. Li, S. Kung, K. P. Jiang and I. M. Conboy, *Nat. Commun.*, 2014, **5**, 4082.
5 A. D. de Araujo, M. Mobli, J. Castro, A. M. Harrington, I. Vetter, Z. Dekan, M. Muttenthaler, J. Wan, R. J. Lewis, G. F. King, S. M. Brierley and P. F. Alewood, *Nat. Commun.*, 2014, **5**, 3165.
6 J. G. Veening, T. R. de Jong, M. D. Waldinger, S. M. Korte and B. Olivier, *Eur. J. Pharmacol.*, 2015, **753**, 209–228.
7 J. Alley, L. M. Diamond, D. L. Lipschitz and K. Grewen, *Psychoneuroendocrinology*, 2019, **106**, 47–56.
8 M. Bellosta-Batalla, M. del Carmen Blanco-Gandía, M. Rodríguez-Arias, A. Cebolla, J. Pérez-Blasco and L. Moya-Albiol, *Stress Health*, 2020, **36**, 469–477.
9 G. Leng and N. Sabatier, *J. Neuroendocrinol.*, 2016, **28**, 1–13.
10 E. A. Lawson, K. E. Ackerman, N. M. Estella, G. Guereca, L. Pierce, P. M. Sluss, M. L. Bouxsein, A. Klibanski and M. Misra, *Eur. J. Endocrinol.*, 2013, **168**, 457–464.
11 A. A. Franke, C. Dabalos, L. J. Custer, X. Li and J. F. Lai, *FASEB J.*, 2019, **33**, 636.
12 N. M. Vizioli, M. L. Rusell and C. N. Carducci, *Anal. Chim. Acta*, 2004, **514**, 167–177.
13 H. Zhou, L. A. Holland and P. Liu, *Analyst*, 2001, **126**, 1252–1256.
14 H. Klauk, *Chem. Soc. Rev.*, 2010, **39**, 2643–2666.
15 T. Minamiki, T. Minami, Y.-P. Chen, T. Mano, Y. Takeda, K. Fukuda and S. Tokito, *Commun. Mater.*, 2021, **2**, 8.
16 T.-T. Huang and W. Wu, *Adv. Mater. Interfaces*, 2020, **7**, 2000015.

17 S. Yuvaraja, A. Nawaz, Q. Liu, D. Dubal, S. G. Surya, K. N. Salama and P. Sonar, *Chem. Soc. Rev.*, 2020, **49**, 3423–3460.
18 J. Wang, D. Ye, Q. Meng, C.-a. Di and D. Zhu, *Adv. Mater. Technol.*, 2020, **5**, 2000218.
19 C. Liao and F. Yan, *Polym. Eng. Rev.*, 2013, **53**, 352–406.
20 F. X. Werkmeister, T. Koide and B. A. Nickel, *J. Mater. Chem. B*, 2016, **4**, 162–168.
21 T. Minami, T. Sato, T. Minamiki, K. Fukuda, D. Kumaki and S. Tokito, *Biosens. Bioelectron.*, 2015, **74**, 45–48.
22 B. Piro, D. Wang, D. Benaoudia, A. Tibaldi, G. Anquetin, V. Noël, S. Reisberg, G. Mattana and B. Jackson, *Biosens. Bioelectron.*, 2017, **92**, 215–220.
23 Q. Zhou, M. Wang, S. Yagi and T. Minami, *Nanoscale*, 2021, **13**, 100–107.
24 L. Zhang, G. Wang, D. Wu, C. Xiong, L. Zheng, Y. Ding, H. Lu, G. Zhang and L. Qiu, *Biosens. Bioelectron.*, 2018, **100**, 235–241.
25 L. Zhang, Z. Liu, C. Xiong, L. Zheng, Y. Ding, H. Lu, G. Zhang and L. Qiu, *Org. Electron.*, 2018, **61**, 254–260.
26 Z. Iskierko, K. Noworyta and P. S. Sharma, *Biosens. Bioelectron.*, 2018, **109**, 50–62.
27 M. Jang, H. Kim, S. Lee, H. W. Kim, J. K. Khedkar, Y. M. Rhee, I. Hwang, K. Kim and J. H. Oh, *Adv. Funct. Mater.*, 2015, **25**, 4882–4888.
28 H. Li, W. Shi, J. Song, H.-J. Jang, J. Dailey, J. Yu and H. E. Katz, *Chem. Rev.*, 2019, **119**, 3–35.
29 C. Sun, X. Wang, M. A. Auwalu, S. Cheng and W. Hu, *EcoMat*, 2021, **3**, e12094.
30 A. Spanu, L. Martines and A. Bonfiglio, *Lab Chip*, 2021, **21**, 795–820.
31 T. Minami, Y. Sasaki, T. Minamiki, S.-i. Wakida, R. Kurita, O. Niwa and S. Tokito, *Biosens. Bioelectron.*, 2016, **81**, 87–91.
32 T. Minamiki, T. Minami, R. Kurita, O. Niwa, S.-i. Wakida, K. Fukuda, D. Kumaki and S. Tokito, *Appl. Phys. Lett.*, 2014, **104**, 243703.
33 N. Bukar, S. S. Zhao, D. M. Charbonneau, J. N. Pelletier and J.-F. Masson, *Chem. Commun.*, 2014, **50**, 4947–4950.
34 P. S. Stayton, S. Freitag, L. A. Klumb, A. Chilkoti, V. Chu, J. E. Penzotti, R. To, D. Hyre, I. Le Trong, T. P. Lybrand and R. E. Stenkamp, *Biomol. Eng.*, 1999, **16**, 39–44.
35 M. Wilchek and E. A. Bayer, *Methods Enzymol.*, 1990, **184**, 5–13.
36 T. Okamoto, C. Mitsui, M. Yamagishi, K. Nakahara, J. Soeda, Y. Hirose, K. Miwa, H. Sato, A. Yamano, T. Matsushita, T. Uemura and J. Takeya, *Adv. Mater.*, 2013, **25**, 6392–6397.
37 K. Haase, C. Teixeira da Rocha, C. Hauenstein, Y. Zheng, M. Hambsch and S. C. B. Mannsfeld, *Adv. Electron. Mater.*, 2018, **4**, 1800076.
38 N. Herzer, S. Hoeppener and U. S. Schubert, *Chem. Commun.*, 2010, **46**, 5634–5652.
39 S. Tatara, Y. Kuzumoto and M. Kitamura, *Jpn. J. Appl. Phys.*, 2016, **55**, 03DD02.
40 T. Minamiki, T. Minami, Y. Sasaki, R. Kurita, O. Niwa, S.-i. Wakida and S. Tokito, *Anal. Sci.*, 2015, **31**, 725–728.
41 O. Azzaroni, M. E. Vela, G. Andreasen, P. Carro and R. C. Salvarezza, *J. Phys. Chem. B*, 2002, **106**, 12267–12273.
42 T. Minami, T. Minamiki, Y. Hashima, D. Yokoyama, T. Sekine, K. Fukuda, D. Kumaki and S. Tokito, *Chem. Commun.*, 2014, **50**, 15613–15615.
43 P. Bergveld, *Sens. Actuators, B*, 2003, **88**, 1–20.
44 J. N. Miller and J. C. Miller, *Statistics and Chemometrics for Analytical Chemistry*, Pearson/Prentice Hall, Upper Saddle River, N.J., 2005.
45 J. Martin, S. M. Kagerbauer, J. Gempt, A. Podtschaske, A. Hapfelmeier and G. Schneider, *J. Neuroendocrinol.*, 2018, **30**, e12596.
46 T. Fujii, J. Schug, K. Nishina, T. Takahashi, H. Okada and H. Takagishi, *Sci. Rep.*, 2016, **6**, 38662.
47 R. White-Traut, K. Watanabe, H. Pournajafi-Nazarloo, D. Schwertz, A. Bell and C. S. Carter, *Dev. Psychobiol.*, 2009, **51**, 367–373.